Phys Chem Minerals (1999) 26: 425–431

ORIGINAL PAPER

M. Ito · H. Yurimoto · M. Morioka · H. Nagasawa

Co^{2+} and Ni^{2+} diffusion in olivine determined by secondary ion mass spectrometry

Received: 1 July 1998 / Revised, accepted: 17 October 1998

Abstract Diffusion coefficients of Co^{2+} and Ni^{2+} in synthetic single crystal forsterite along the *c*-axis were determined in the temperature ranges, 700–1200 °C and 800–1300 °C, respectively. The synthesized forsterite specimens were coated with thin evaporated films of CoO and NiO on the *c*-surface and annealed for diffusion experiments. The short penetration distance of diffusing ions in forsterite was measured by secondary ion mass spectrometry using the depth profile method. The diffusion coefficients of Co (700–1200 °C) and Ni (800–1300 °C) are given by:

$$D_{\mathrm{Co}} = 5.59 \times 10^{-5}[\mathrm{m^2 s^{-1}}] \exp\left(\frac{-328 \pm 40\ [\mathrm{kJmol^{-1}}]}{RT}\right)$$

and

$$D_{\mathrm{Ni}} = 1.45 \times 10^{-2}[\mathrm{m^2 s^{-1}}] \exp\left(\frac{-392 \pm 17\ [\mathrm{kJmol^{-1}}]}{RT}\right).$$

The observed diffusion coefficient values show good linear relationships in Arrhenius plots and the activation energy values obtained agree well with the previous values, although the diffusion coefficient values observed at the high temperature end of the experimental range deviate from the previous values. These results indicate that Co and Ni diffuse in olivine with a single mechanism within the temperature range observed, possibly with an extrinsic in nature as in the case of Mg tracer diffusion observed by Chakraborty et al. 1994 and of Fe-Mg interdiffusion by Chakraborty.

Key words SIMS · Depth profiling · Forsterite Diffusion · Arrhenius plot · Activation energy

M. Ito (✉) · H. Nagasawa
Faculty of Science, Department of Chemistry,
Gakushuin University, Mejiro, Toshima-ku,
Tokyo 171-8588, Japan
e-mail: motoo.ito@gakushuin.ac.jp

H. Yurimoto
Department of Earth and Planetary Sciences,
Tokyo Institute of Technology, Ookayama,
Meguro-ku, Tokyo 152-8551, Japan

M. Morioka
Radioisotope Centre, University of Tokyo,
Yayoi, Bunkyo-ku, Tokyo 113-0032, Japan

Introduction

The diffusion study of silicate minerals in the field of geochemistry has substantial significance in understanding thermal histories, rheological properties, rate of reactions such as oxidation, site exchange, phase changes etc. in rocks and minerals. Diffusion coefficients in olivine, in particular, are necessary for investigating models and processes in the Earth's mantle and meteorite parent bodies. For example, they are used to estimate the rate of creep deformation of olivine, which strongly constrains the transport of materials in the Earth's upper mantle, and to construct models that fit the observed compositional zoning profiles in olivine to understand cooling rates and thermal histories of meteorites. For these reasons, the measurement of diffusion coefficients in olivine has been performed by various workers (e.g. Clark and Long 1971; Misener 1972, 1974; Buening and Buseck 1973; Morioka 1980, 1981, 1983; Jaoul et al. 1980, 1981, 1983; Hermeling and Schmalzried 1984; Nakamura and Schmalzried 1984; Andersson et al. 1989; Yurimoto et al. 1992; Chakraborty et al. 1994; Jaoul et al. 1995; Nagasawa and Morioka 1996; Chakraborty 1997).

Until recently, diffusion coefficients in olivine have been measured using conventional methods, namely the radioactive tracer method (e.g., Morioka 1981, 1983; Hermeling and Schmalzried 1984) and the couple annealing method combined with electron microprobe analysis (e.g., Buening and Buseck 1973; Misener 1972, 1974; Morioka 1980, 1981; Nakamura and Schmalzried 1984; Nagasawa and Morioka 1996; Chakraborty 1997).

In these studies, diffusion coefficients were obtained above about 1000 °C because of experimental limitations. However, in natural systems (transition temperature of the mantle, temperature of reheating of meteorite etc.), diffusion occurs frequently below 1000 °C. In order to apply the observed values to the natural processes, it is necessary to extrapolate the results observed above 1000 °C to the lower temperature. Recent developments of secondary ion mass spectrometry (SIMS) have enabled measurement of diffusion coefficients of cations at relatively low temperature. By using the depth profile method by SIMS, it is possible to determine diffusion coefficients from penetration distance of less than 1 μm. For example, Yurimoto et al. (1989, 1992) reported oxygen diffusion in olivine and melilite, Chakraborty et al. (1994) determined Mg tracer diffusion in olivine and Schwandt et al. (1993, 1995) measured Mg self-diffusion in garnet using the thin film technique.

The Fe-Mg interdiffusion coefficient is very important for geo- and cosmochemistry. A number of studies have reported Fe-Mg diffusion in olivine (e.g. Misener 1972, 1974; Buening and Buseck 1973; Hermeling and Schmalzried 1984; Nakamura and Schmalzried 1984; Jaoul et al. 1995; Chakraborty 1997). However, since control of the partial pressure of oxygen is a crucial factor for determining diffusion coefficient (Buening and Buseck 1973), considerable difficulties are associated with not only the Fe-Mg interdiffusion measurement, but also with theoretically constructing the thermal history of the sample. In this respect Co^{2+} and Ni^{2+} are easier ionic species to handle in diffusion measurements since they are believed to be less sensitive to the partial pressure of oxygen, although a small amount of Fe-impurity may affect Co and Ni diffusion. Diffusional behavior of Co^{2+} and Ni^{2+} at lower temperatures, if known, would provide important information on the diffusional behavior of Fe-Mg under low temperature conditions. In addition, if distribution profiles of minor or trace elements, such as Co and Ni, in natural olivine in meteorites, etc., are determined by SIMS, diffusion coefficients for Co^{2+} and Ni^{2+} should be useful in elucidating thermal histories of the samples. Thus, we have chosen Co^{2+} and Ni^{2+} to examine the diffusion properties of cations in olivine in the low temperature region below 1000 °C.

In this work SIMS was used to measure diffusion profiles obtained at annealing temperatures below 1000 °C. Very high spatial resolution obtained by the use of SIMS depth profiling enabled the determination of diffusion coefficients below 1000 °C, where the penetration distance of the diffusing ion is normally <500 nm.

Experimental procedure

A single crystal of forsterite grown by the Czochralski method was used. The starting materials, MgO and SiO_2, supplied by Wako Pure Chemical Co. and quality better than 3N, were weighed in the correct stoichiometric proportions for Mg_2SiO_4. The mixed material was preheated at 1000 °C for 2 h in air and then loaded into an Ir crucible. In order to protect the crucible from oxidation, a continuous gas flow of N_2 at a rate of 200–300 ml/min was introduced during the forsterite crystal growth. The growth conditions were the same as previously reported by Morioka (1980). A good quality forsterite crystal, free from visible internal imperfections such as cracks, gas bubbles and any other inclusions, was pulled along the *a*-axis at a rate of 3 mm/h and rotation rate of 10 rpm. The crystal obtained was 30 mm in diameter and 80 mm in length.

The crystal was cut into small slabs with a 5 mm square surface perpendicular to the *c*-axis and 1 mm in thickness with a diamond saw. The surface of the slab was polished with 15 to 0.25 μm diamond paste and finished with 0.05 μm alumina paste to obtain the necessary surface flatness. After polishing, the *c*-surface (perpendicular to [001]) of the forsterite samples were coated with a thin evaporated film (~20 nm) of CoO or NiO. The samples, enveloped in a Pt foil (0.1 mm thickness), were annealed in air in a resistance furnace from 120 s (1200 °C) to 1000 h (700 °C) for Co diffusion, and from 120 s (1300 °C) to 720 h (800 °C) for Ni diffusion (Table 1). Diffusion annealing experiments of high temperature, 1200–1300 °C, were conducted for duration of 110–200 s. The sample in a Pt foil was placed in a low temperature area of the furnace, and moved quickly to the high temperature area. After the annealing, the sample was rapidly removed from the furnace. The annealing time was selected to obtain penetration distance of at least 0.1 μm to minimize the error resulting from the uncertainty in position of the evaporated thin film-forsterite crystal interface. The annealing temperature was measured with a Pt-Pt · Rh thermocouple, and regulated by a PID control system. The temperature fluctuations were within ±3 °C of the set annealing temperature.

The diffusion profiles of Co and Ni, secondary ion intensities versus penetration distance into the annealed samples, were determined by SIMS (CAMECA, IMS-3f) using the depth profiling method at Tokyo Institute of Technology. The basic measurement conditions have been described in detail in the previous work (Yurimoto et al. 1992).

The primary ion beam was mass filtered negative ^{16}O accelerated to 12.5 keV with a beam current of 60 to 100 nA and a beam spot size of 50 to 80 μm diameter. The primary ion beam was rastered about 300 to 500 μm square during analyses. Electrostatic charging on the samples by the primary ion beam was virtually eliminated by 25 nm of gold film evaporated on the sample surface. The intensities of the positive secondary ions were measured by offsetting the sample accelerating voltage (−50 for Ni and −100 V for Co) and the energy band-pass was set to 20 eV. The flat-bottomed final crater depth was measured using an optical interferometer. These conditions produced a linear sputter rate of 63 ± 2 pms^{-1}.

Secondary ions were extracted at a voltage of 4500 V, and were collected the central 60 μm of the sputtered area using a mechanical aperture in order to minimize artifacts arising from crater edge effects and redeposition of evaporated materials. Counts of secondary ions were obtained as functions of time. The ^{26}Mg, ^{30}Si, and ^{59}Co for Co diffusion and ^{26}Mg, ^{30}Si, ^{58}Ni, and ^{60}Ni for Ni diffusion were monitored during primary beam sputtering.

Results

A typical depth profile is shown in Fig. 1a. Diffusion coefficients were calculated by a diffusion model that provided the best fit to the depth profiles. Diffusion coefficients were calculated using a thin-film diffusion model solution to the Fickian diffusion equations (e.g. Crank 1975).

$$c(x) = \frac{M}{\sqrt{4\pi Dt}} \exp\left(\frac{-x^2}{4Dt}\right) \quad (1)$$

Table 1 Co and Ni diffusion coefficients along *c*-axis in single crystal forsterite

Temperature (°C)	Anneal time	D^a for Co (m^2s^{-1})
1200	120 s	$1.94 \pm 1.48 \times 10^{-16}$ [b]
	200 s	$6.03 \pm 1.58 \times 10^{-16}$
		Weighted mean $3.86 \pm 1.08 \times 10^{-16}$
1100	10 800 s (3 h)	Average $2.02 \pm 2.06 \times 10^{-17}$
1050	23 400 s (6.5 h)	$3.54 \pm 0.29 \times 10^{-18}$
	50 400 s (14 h)	$4.81 \pm 0.30 \times 10^{-18}$
		Weighted mean $4.80 \pm 0.21 \times 10^{-18}$
1000	19 800 s (5.5 h)	$4.72 \pm 2.61 \times 10^{-18}$
	72 000 s (20 h)	$1.77 \pm 0.72 \times 10^{-18}$
	90 000 s (25 h)	$1.28 \pm 0.79 \times 10^{-18}$
		Weighted mean $1.68 \pm 0.52 \times 10^{-18}$
900	144 000 s (40 h)	$3.52 \pm 0.32 \times 10^{-20}$
	504 000 s (140 h)	$5.68 \pm 3.17 \times 10^{-20}$
		Weighted mean $3.54 \pm 0.32 \times 10^{-20}$
800	385 200 s (107 h)	$1.31 \pm 0.21 \times 10^{-21}$
	720 000 s (200 h)	$6.75 \pm 1.16 \times 10^{-21}$
		Weighted mean $1.47 \pm 0.20 \times 10^{-21}$
700	900 000 s (250 h)	$5.19 \pm 1.36 \times 10^{-22}$
	3 600 000 s (1000 h)	$4.83 \pm 2.98 \times 10^{-22}$
		Weighted mean $5.13 \pm 1.24 \times 10^{-22}$

[a] *D*, calculated from profile of $^{59}Co/^{30}Si$
[b] Standard deviation obtained from several independent SIMS measurements

Temperature (°C)	Anneal time	D^a for Ni (m^2s^{-1})
1300	120 s	Average $7.66 \pm 0.88 \times 10^{-16}$ [b]
1200	110 s	$1.96 \pm 0.48 \times 10^{-16}$
	200 s	$6.73 \pm 4.43 \times 10^{-16}$
		Weighted mean $2.01 \pm 0.48 \times 10^{-18}$
1100	900 s (15 min)	$3.15 \pm 0.84 \times 10^{-17}$
	5760 s (1.6 h)	$1.13 \pm 0.35 \times 10^{-17}$
	9720 s (2.7 h)	$5.25 \pm 2.70 \times 10^{-17}$
		Weighted mean $1.49 \pm 0.32 \times 10^{-17}$
1050	21 600 s (6 h)	$7.85 \pm 0.22 \times 10^{-18}$
	25 200 s (7 h)	$1.41 \pm 0.36 \times 10^{-18}$
		Weighted mean $6.04 \pm 1.88 \times 10^{-18}$
1000	79 200 s (22 h)	$7.14 \pm 5.14 \times 10^{-19}$
	172 800 s (48 h)	$8.77 \pm 2.82 \times 10^{-19}$
		Weighted mean $8.39 \pm 2.47 \times 10^{-19}$
900	1 584 000 s (440 h)	$8.71 \pm 0.43 \times 10^{-20}$
	1 900 800 s (528 h)	$1.64 \pm 0.21 \times 10^{-19}$
		Weighted mean $9.01 \pm 0.42 \times 10^{-20}$
800	2 592 000 s (720 h)	Average $6.99 \pm 5.86 \times 10^{-22}$

[a] *D*, calculated from profile of $^{58}Ni/^{30}Si$ and $^{60}Ni/^{30}Si$
[b] Standard deviation obtained from several independent SIMS measurements

where $c(x)$ is the concentration at a depth x, M is the total amount of source of diffusion, D is the diffusion coefficient, t is the duration of the anneal. The equation represents a homogeneous penetration of cations into forsterite. The log of the intensity ratio, $^{59}Co/^{30}Si$, is plotted as a function of the square of the penetration distance in Fig. 1b. According to Eq. (1), this should yield a linear array. A slope equal to $1/(4\,Dt)$ was computed by least-square fitting and diffusion coefficients were calculated (Table 1). In the Ni diffusion experiments both ^{58}Ni and ^{60}Ni profiles were measured (Fig. 1c). Based on the similarity in the diffusion profiles observed, both isotopes were found to have essentially the same mobility in the experiments. Ni diffusion coefficients listed in Table 1 are those calculated from the diffusion profiles of ^{58}Ni, which is the major isotope of Ni.

Diffusion experiments were conducted for several different durations (Table 1) at each temperature to ensure that the diffusion coefficients are independent of time. Some of the values measured at a given temperature obtained by fitting a diffusion profile to Eq. (1) show deviations which are considerably larger than the standard deviations calculated from the results of repeated SIMS analysis (3–5 times for each sample). Inadequate long or short annealing time caused larger errors. For example, 200 s annealing experiment at 1200 °C in Ni diffusion experiment (Table 1) showed a larger error compared with the 110 s experiment. Since approximately the same amount of Ni was deposited on the surface of the sample in these experiments, the longer annealing time resulted in deeper penetration of Ni in the sample, producing lower concentrations of Ni in each measurement with larger errors of determination.

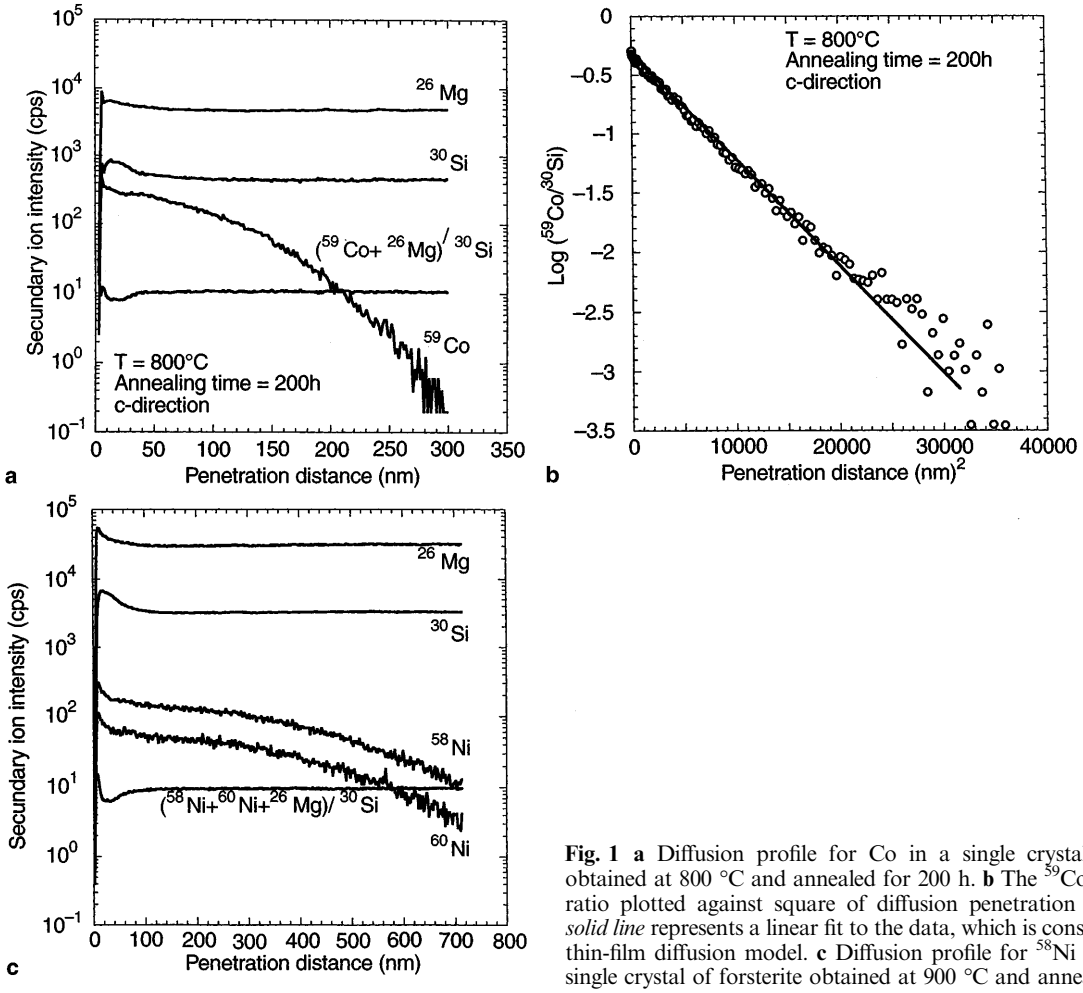

Fig. 1 **a** Diffusion profile for Co in a single crystal of forsterite obtained at 800 °C and annealed for 200 h. **b** The ^{59}Co/^{30}Si intensity ratio plotted against square of diffusion penetration distance. The *solid line* represents a linear fit to the data, which is consistent with the thin-film diffusion model. **c** Diffusion profile for ^{58}Ni and ^{60}Ni in a single crystal of forsterite obtained at 900 °C and annealed for 440 h

Too short an annealing time, on the other hand, produces large errors due to uncertainty in determining the diffusion profile with too short penetration. A major source of these deviations appears to be in the systematic errors produced by estimation of the diffusion interface. According to Schwandt et al. (1993), an apparent annealing time-dependence on the diffusion was caused by the surface effect when annealing time is insufficiently short. Thus it is necessary to determine properly the position of diffusion interface ($x = 0$), which is a critical parameter for calculating diffusion coefficients. The interface was determined by examining the (^{59}Co + ^{26}Mg)/^{30}Si intensity ratio for Co diffusion and the (^{58}Ni + ^{60}Ni + ^{26}Mg)/^{30}Si intensity ratio for Ni diffusion, which must be constant within the forsterite crystal. By this treatment possible effects of sputtering of Au thin film, a few nm order of non-stoichiometric layer produced by vapor deposition of diffusing element etc. on near the sample surface can be omitted in the calculation of diffusion coefficients. The ^{30}Si intensity is used as a reference to reduce or eliminate any variations in the secondary ion intensities from the SIMS analysis, because of ^{30}Si is a constant component in forsterite. The uncertainty in the position of the thin film-forsterite interface is normally less than ±20 nm, which translates to an uncertainty D of +30% to −15%, for a diffusion coefficient value measured under appropriate annealing time. For abnormal values standard deviations determined from replicate analyses are usually larger than the normal cases. Thus the average diffusion coefficient values shown in Table 1 were calculated as the weighted mean in which inverse of the square of the standard deviation from multiple measurement is taken as the weight.

Discussion

The annealing time for an experiment at 1200–1300 °C was relatively short, about 110–200 s. To minimize the uncertainty over the annealing time, the sample which had been placed in a low temperature part of the furnace was quickly moved to the high temperature part, observed until the designated temperature was reached and then the sample was quickly removed from the high temperature part of the furnace at the end of the annealing time. Considering that the change of temperature in the furnace was not observed by a thermocouple,

and the heat capacity of the furnace is significantly larger than that of the sample, the error in the annealing time should be less than a few seconds.

The temperature dependence of the Co and Ni diffusion coefficient in forsterite can be presented in terms of Arrhenius plot, or Log D vs. $1/T$, which is shown in Fig. 2. The Arrhenius relationship is typically defined in Eq. (2), which can be rewritten in Eq. (3) as:

$$D = D_0 \exp\left(\frac{-E}{RT}\right), \tag{2}$$

and,

$$\text{Log } D = \text{Log } D_0 - \frac{E}{2.303RT}, \tag{3}$$

where D is the diffusion coefficient, D_0 is the preexponential factor, E is the activation energy for diffusion, T is the absolute temperature (K) and R is the gas constant. The slope of the best-fit line to Eq. (3) provides the value of the activation energy, E, expressed in kJ mol^{-1}. Co diffusion in forsterite provides 328 ± 40 kJ mol^{-1} (annealing temperature range: 700–1200 °C) and $D_0 = 5.59 \times 10^{-5}$ m^2 s^{-1}. Ni diffusion in forsterite provides 392 ± 17 kJ mol^{-1} (annealing temperature range: 800–1300 °C) and $D_0 = 1.45 \times 10^{-2}$ m^2 s^{-1}. The solid lines in Fig. 2a, b are linear regression fits to the data with correlation coefficients of 0.98 and 0.99 for Co and Ni, respectively.

As shown in Fig. 2a, b, Co and Ni data each plot on a single Arrhenius curve indicating that a single diffusion mechanism is operative in each case under these experimental conditions. The Co and Ni diffusion data are presented in an Arrhenius plot with previous results in Fig. 3 and the activation energy values are shown in Table 2. Apart from the values for the low temperature experiment for Fe-Mg interdiffusion (Buening and Buseck 1973) and Ni-Mg interdiffusion (Clark and Long 1971), activation energy values for all ions show good agreement, indicating that all elements diffuse via the same mechanism. It is also shown that the activation energies decrease with increasing ionic radius, namely in the order Mg > Ni > Co > Fe.

The activation energies for Co and Ni diffusion agree well with the previous values (Morioka 1981; Nagasawa and Morioka 1996). The Co values observed at 1200 °C are lower and the Ni values at 1300 °C are higher compared with the previous values (Nagasawa and Morioka 1996). However, when compared with Morioka (1981), the Arrhenius relation is quite similar to our results. The reason for these discrepancies is uncertain, but may due to differences in the conditions of the single crystal specimens. In defect-mediated diffusion

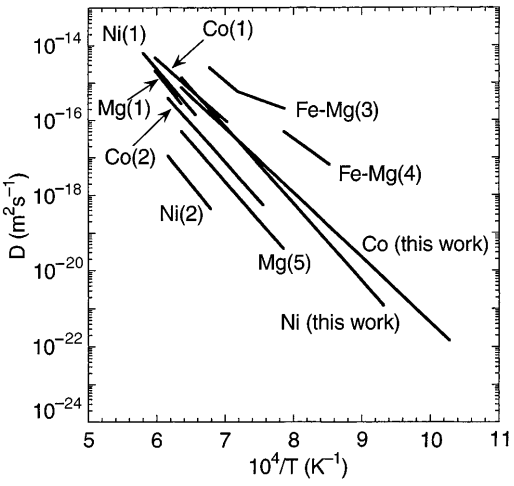

Fig. 3 Comparison of Arrhenius relations obtained from various studies on cation diffusion in forsterite. The values are calculated from extrapolated values for pure forsterite. *1*, Morioka (1981); *2*, Nagasawa and Morioka (1996); *3*, Buening and Buseck (1973); *4*, Misener (1974); and *5*, Chakraborty et al. (1994)

Fig. 2a, b Arrhenius plot (Log D versus $1/T$) for diffusion of **a** Co and **b** Ni in a single crystal of forsterite. The correlation coefficients for these Arrhenius relations are 0.98 and 0.99 for Co and Ni, respectively. Error bars represent standard deviation estimated from repeated SIMS analyses

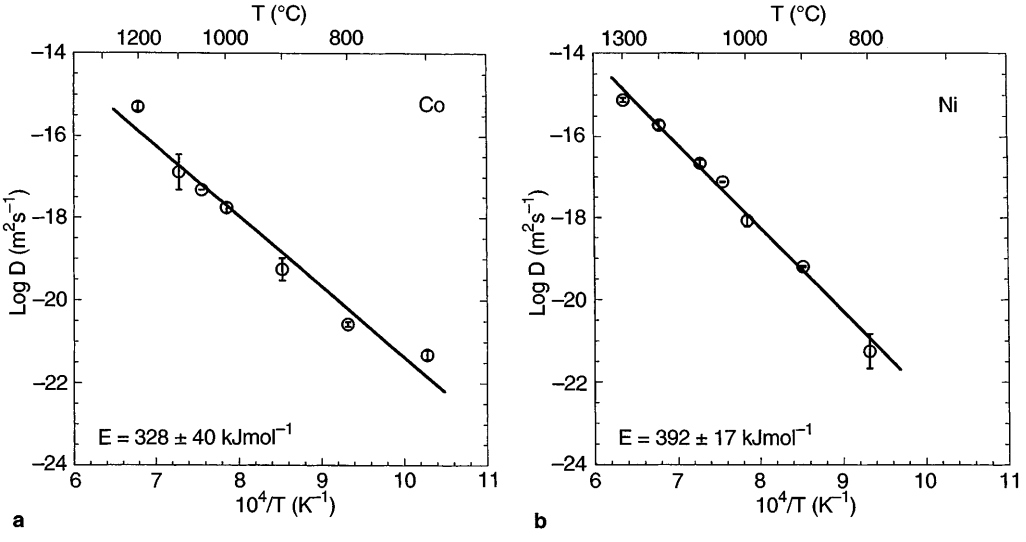

Table 2 Calculated activation energies, E, for some divalent cation diffusion in forsterite. The values of Co, Ni, Fe and Mg are calculated from extrapolated values for forsterite

Divalent cations	Literature	Temperature (°C)	E (kJ/mol)
Co	Morioka (1980, 1981)	1150 ~ 1450	313
	Nagasawa and Morioka (1996)	1050 ~ 1350	393
	This work	700 ~ 1200	328
Ni	Clark and Long (1971)	1149 ~ 1234	193
	Morioka (1981)	1250 ~ 1450	414
	Nagasawa and Morioka (1996)	1200 ~ 1350	431
	This work	800 ~ 1300	392
Fe	Buening and Buseck (1973)	1125 ~ 1200	264
		1000 ~ 1125	133
	Misener (1974)	900 ~ 1000	252
	Chakraborty (1997)	980 ~ 1300	226
Mg	Morioka (1981)	1300 ~ 1400	444
	Chakraborty et al. (1994)	1000 ~ 1300	400

processes, differences in defect densities in the crystal cause differences in diffusivities. Thus, differences in crystal defects due to impurities or frozen defects produced at higher temperature, etc., may cause differences in diffusivities of cations in the crystals because the same growth condition of the crystal cannot be obtained in the crystal with same number of impurities or defects.

It is generally believed that the lattice diffusion of a cation into a mineral crystal structure is controlled by the formation and number of point defects. For example, Lasaga (1981) discussed intrinsic and extrinsic behaviors in minerals, and the importance of point defects for diffusion. In the intrinsic regime at high temperature, point defects are thermally generated and controlled, so that diffusion coefficients are mainly controlled by changes in defect density. At lower temperature, cation impurities affect the point defect density to a greater extent than does the temperature, thereby defining extrinsic behavior. On an Arrhenius plot, steep slopes represent the intrinsic region and gentle slopes represent the extrinsic region (Freer 1981). An Arrhenius plot is therefore useful for illustrating the presence of intrinsic and extrinsic regions. Buening and Buseck (1973) suggested that Fe-Mg interdiffusion in San-Carlos olivine has an intrinsic regime above 1125 °C and an extrinsic regime below 1125 °C. However, Chakraborty (1997) showed that Fe-Mg interdiffusion in olivine has no intrinsic and extrinsic regime on the Arrhenius plot. The observed linearity on the Arrhenius plots of the Co and Ni diffusion data, together with the small deviations between the diffusivities observed in the previous and present work at higher temperature, suggests that a single mechanism, possibly of extrinsic origin, operates in the measured temperature range for both Co and Ni. This conclusion is consistent with the results for Mg tracer diffusion observed by Chakraborty et al. (1994) at temperatures of 1000–1300 °C and for Fe-Mg interdiffusion by Chakraborty (1997) at 980–1300 °C.

If the results of this work and those of Chakraborty et al. (1994) indicate that diffusion of each divalent cation in olivine occurs by a single extrinsic mechanism, it is highly possible that Fe-Mg interdiffusion also occurs by a similar mechanism and the Fe-Mg interdiffusion coefficients measured at high temperatures can be extrapolated to lower temperatures, e.g., below 1000 °C. In fact, Chakraborty (1997) indicated an important point that there is no change of diffusion mechanism (no kink of the Arrhenius plot) and, thus it should be possible to extrapolate Fe-Mg interdiffusion to the lower temperature.

Conclusion

It has been shown that divalent Co and Ni ions diffuse in olivine by a single diffusion mechanism in the temperature ranges 700–1200 °C and 800–1300 °C, respectively. A very important finding is that there is no kink in the Arrhenius plot over the wide temperature range, which indicates the diffusion data may be extrapolated to low temperatures fairly safely. Chakraborty (1997) showed that there is no break in Arrhenius plot and that the Fe-Mg interdiffusion coefficient values measured at high temperatures can be extrapolated to lower temperatures. Thus, Fe^{2+} in forsterite diffuses in the olivine structure by a mechanism similar to those for Co and Ni. The results of Co and Ni diffusion data cannot be directly applied for geospeedmetry because of the effect of Fe in natural olivine. However, it may be useful in elucidating thermal histories of geo- and cosmochemical samples, if concentration gradients of these elements are observed in olivine in these samples.

Acknowledgements We are grateful to Dr. T. LaTourrette of UCLA for criticizing the draft of this paper. Critical reviews by Dr. O. Jaoul and Dr. S. Chakraborty improved this manuscript considerably. A part of this study is supported by a grant in aid by the Ministry of Education 09451377 and by the Science and Technology Agency of the Japanese Government.

References

Andersson K, Borchardt G, Scherrer S, Weber S (1989) Self diffusion in Mg_2SiO_4 (forsterite) at high temperature: a model case study for SIMS analysis on ceramic surface. Fresenius Z Anal Chem 333: 383–385

Buening DK, Buseck PR (1973) Fe-Mg lattice diffusion in olivine. J Geophy Res 78: 6852–6862

Chakraborty S (1997) Rates and mechanisms of Fe-Mg interdiffusion in olivine at 980–1300 °C. J Geophys Res B6 102: 12317–12331

Chakraborty S, Farver JR, Yund RA, Rubie DC (1994) Mg tracer diffusion in synthetic forsterite and San Carlos olivine as a function of P, T and fO_2. Phys Chem Minerals 21: 489–500

Clark AM, Long JVP (1971) Anisotoropic diffusion in olivine. In: Thomas Graham Memorial Symposium on Diffusion Processes, pp 511–521

Crank J (1975) The mathematics of diffusion. Oxford University Press, London

Freer R (1981) Diffusion in silicate minerals and glasses: a data digest and guide to the literature. Contrib Mineral Petrol 76: 440–454

Hermeling J, Schmalzried H (1984) Tracer diffusion of the Fe-cations in olivine $(Fe_xMg_{1-x})_2SiO_4$ (III). Phys Chem Minerals 11: 161–166

Jaoul O, Froidevaux C, Durham WB, Michaut M (1980) Oxygen self-diffusion in forsterite: Implication for the high temperature creep mechanism. Earth Planet Sci Lett 47: 391–397

Jaoul O, Poumellec M, Froidevaux C, Havette A (1981) Silicon diffusion in forsterite: A new constraint for understanding mantle deformation. In: Stacy ED et al. (eds) Anelasticity in the Earth. pp 95–100 Geodyn Ser vol 4, Am Geophys Union, Washington, DC

Jaoul O, Houlier B, Abel F (1983) Study of ^{18}O diffusion in magnesium orthosilicate by nuclear microanalysis. J Geophys Res 88: 613–624

Jaoul O, Bertran-Alvarez Y, Liebermann RC, Price GD (1995) Fe-Mg interdiffusion in olivine up to 9 GPa at T = 600–900 °C; experimental data and comparison with defect calculations. Phys Earth Planet Inter 89: 199–218

Lasaga AC (1981) The atomistic basis of kinetics: defects in minerals. In: Mineral Soc Am Reviews in Mineralogy 8: 216–319

Misener DJ (1972) Interdiffusion studies in the system Fe_2SiO_4-Mg_2SiO_4. Carnegie Inst Yearbook 71: 516–520

Misener DJ (1974) Cationic diffusion in olivine to 1400 °C and 35 kbar. In: Hofmann AW et al. (eds) Geochemical transport and kinetics. pp 117–129

Morioka M (1980) Cation diffusion in olivine-I. Cobalt and magnesium. Geochim Cosmochim Acta 44: 759–762

Morioka M (1981) Cation diffusion in olivine-II. Ni-Mg, Mn-Mg, Mg and Ca. Geochim Cosmochim Acta 45: 1573–1580

Morioka M (1983) Cation diffusion in olivine-III. Mn_2SiO_4 system. Geochim Cosmochim Acta 47: 2275–2279

Nagasawa H, Morioka M (1996) Synthesis and diffusion measurement of double-layered single crystals of olivine. Chikyukagaku (Geochemistry) 30: 17–25

Nakamura A, Schmalzried H (1984) On the Fe^{2+}-Mg^{2+}-interdiffusion in olivine (II). Ber Bunsenges Phys Chem 88: 140–145

Schwandt CS, Cygan RT, Westrich HR (1993) A thin film approach for producing mineral diffusion couples. PAGEOPH 141: 631–64

Schwandt CS, Cygan RT, Westrich HR (1995) Mg self-diffusion in pyrope garnet. Am Mineral 80: 483–490

Yurimoto H, Morioka M, Nagasawa H (1989) Diffusion in single crystals of melilite: I. Oxygen. Geochim Cosmochim Acta 53: 2387–2394

Yurimoto H, Morioka M, Nagasawa H (1992) Oxygen self-diffusion along high diffusivity paths in forsterite. Geochem J 26: 181–188